Title
Can pore-clogging by ash explain post-fire runoff?

Journal
International Journal of Wildland Fire, 25(3)

ISSN
1049-8001

Authors
Stoof, Cathelijne R
Gevaert, Anouk I
Baver, Christine
et al.

Publication Date
2016

DOI
10.1071/wf15037

Peer reviewed

CSIRO PUBLISHING

International Journal of Wildland Fire **2016**, *25*, 294–305
http://dx.doi.org/10.1071/WF15037

Can pore-clogging by ash explain post-fire runoff?

Cathelijne R. Stoof[A,B,I], *Anouk I. Gevaert*[A,C,D], *Christine Baver*[A], *Bahareh Hassanpour*[A], *Verónica L. Morales*[E,F], *Wei Zhang*[G], *Deborah Martin*[H], *Shree K. Giri*[A] *and Tammo S. Steenhuis*[A]

[A]Department of Biological and Environmental Engineering, Riley Robb Hall, Cornell University, Ithaca, NY 14853, USA.
[B]Soil Geography and Landscape Group, Wageningen University, PO Box 47, 6700 AA Wageningen, the Netherlands.
[C]Hydrology and Quantitative Water Management Group, Wageningen University, PO Box 47, 6700 AA Wageningen, the Netherlands.
[D]Earth and Climate Cluster, Department of Earth Sciences, VU University, De Boelelaan 1085, 1081 HV Amsterdam, the Netherlands.
[E]SIMBIOS Centre, Abertay University, Dundee DD1 1HG, United Kingdom.
[F]Institute of Environmental Engineering, ETH Zürich, Zürich 8093, Switzerland.
[G]Department of Plant, Soil and Microbial Sciences, Environmental Science and Policy Program, Michigan State University, 1066 Bogue Street, East Lansing, MI 48824, USA.
[H]United States Geological Survey, 3215 Marine Street (E147), Boulder, CO 80303-1066, USA.
[I]Corresponding author. Email: cathelijne.stoof@wur.nl

Abstract. Ash plays an important role in controlling runoff and erosion processes after wildfire and has frequently been hypothesised to clog soil pores and reduce infiltration. Yet evidence for clogging is incomplete, as research has focussed on identifying the presence of ash in soil; the actual flow processes remain unknown. We conducted laboratory infiltration experiments coupled with microscope observations in pure sands, saturated hydraulic conductivity analysis, and interaction energy calculations, to test whether ash can clog pores (i.e. block pores such that infiltration is hampered and ponding occurs). Although results confirmed previous observations of ash washing into pores, clogging was not observed in the pure sands tested, nor were conditions found for which this does occur. Clogging by means of strong attachment of ash to sand was deemed unlikely given the negative surface charge of the two materials. Ponding due to washing in of ash was also considered improbable given the high saturated conductivity of pure ash and ash–sand mixtures. This first mechanistic step towards analysing ash transport and attachment processes in field soils therefore suggests that pore clogging by ash is unlikely to occur in sands. Discussion is provided on other mechanisms by which ash can affect post-fire hydrology.

Additional keywords: hydraulic conductivity, infiltration, wildland fire ash.

Received 6 February 2015, accepted 21 October 2015, published online 20 January 2016

Introduction

Worldwide, forest and other land-clearing fires affect 3.4 million km^2 annually (Giglio *et al.* 2010), causing economic and ecological impacts. Land degradation is one common effect of fire (Shakesby and Doerr 2006; Cerdà and Robichaud 2009; Moody *et al.* 2013), because of increased surface runoff and erosion due to combined effects of heat-induced soil physical changes, soil surface changes and vegetation removal (Meixner and Wohlgemuth 2003; Hubbert *et al.* 2006; Stoof *et al.* 2012). Ash plays an additional important role in controlling runoff and erosion processes (Kutiel *et al.* 1995; Onda *et al.* 2008; Woods and Balfour 2008; Bodí *et al.* 2014), and the type and magnitude of response are a function of ash thickness, type, crusting potential, and hydraulic conductivity, soil type and rainfall characteristics (Bodí *et al.* 2014). Ash can store rainfall (Nyman *et al.* 2014) and thereby mitigate surface runoff and erosion for a limited period after fire (Cerdà and Doerr 2008; Woods and Balfour 2008; Woods and Balfour 2010; Bodí *et al.* 2012; Ebel *et al.* 2012; León *et al.* 2013), but it is also frequently suggested that clogging of soil pores by ash is a factor in the common increase in runoff and erosion after wildfire (Mallik *et al.* 1984; Etiégni and Campbell 1991; Gabet and Sternberg 2008; Nyman

et al. 2010; Woods and Balfour 2010; Bodí *et al.* 2012; Bodí *et al.* 2014). Evidence for this is lacking, however, as to date, research has primarily focussed on identifying the presence of ash in soil (Woods and Balfour 2010; Stoof *et al.* 2010). As the mere presence of ash in soil does not indicate that it clogs pores and blocks infiltration to the point that runoff or ponding occurs, there is a need to elucidate the flow processes associated with the transport and potential pore clogging of ash. This is important because the occurrence of surface runoff after fire in general, and specifically in ash-on-soil systems, can also be caused by processes other than pore clogging (Bodí *et al.* 2014).

Interest in the fate of ash after fire is high, in part because of its considerable carbon sequestration and water-quality impacts (Smith *et al.* 2011; Santín *et al.* 2012; Audry *et al.* 2014; Costa *et al.* 2014). Ash produced during fire is defined as 'the particulate residue remaining, or deposited on the ground, from the burning of wildland fuels', comprising both partially combusted organic material (char) and mineral components (Bodí *et al.* 2014). The composition of ash varies between plant species, combustion completeness and fire severity (Pereira *et al.* 2012; Balfour and Woods 2013), with a spectrum from black carbon-rich to white carbonate-rich ash being produced with increasing combustion completeness and fire severity (Goforth *et al.* 2005; Balfour and Woods 2013; Dlapa *et al.* 2013). Ash is typically deposited in 0.5–5.0-cm-thick layers (Bodí *et al.* 2014) that can be quickly redistributed after fire by wind and surface runoff (Pereira *et al.* 2015; Pereira *et al.* 2013). Although its potential pore-clogging effect is often used to explain reduced infiltration rates (Etiégni and Campbell 1991; Nyman *et al.* 2010; Woods and Balfour 2010; Bodí *et al.* 2012; Bodí *et al.* 2014), ash that is not crusted can be highly permeable (56–3600 mm h^{-1}; Bodí *et al.* 2014) and can mediate delivery of water to underlying layers (Ebel *et al.* 2012).

That ash may cause pore clogging is a reasonable premise, as issues with pore clogging caused by transport of fine particles into coarser soil are well known in, for instance, wastewater disposal, groundwater extraction and artificial groundwater recharge (Platzer and Mauch 1997; Baveye *et al.* 1998). Pore clogging causes a gradual reduction in saturated hydraulic conductivity of the porous medium to the point that it becomes fully impermeable and ponding occurs, and generally occurs as the combined interaction of physical, chemical and biological factors (Blazejewski and Murat-Blazejewska 1997; Baveye *et al.* 1998): (1) physical clogging is caused by straining and deposition of fines at the surface (De Vries 1972), in pore necks, or at air, water or solid interfaces (McDowell-Boyer *et al.* 1986; Bradford and Torkzaban 2008); (2) chemical clogging is controlled by the attachment and repulsion between colloid-size particles and porous media, with interaction energies governing these processes described as the sum of electrostatic and Van der Waals forces according to Derjaguin–Landau–Verweij–Overbeek (DLVO) theory (Bradford *et al.* 2013); (3) biological clogging, finally, is caused by microbial growth (Baveye *et al.* 1998).

We tested the hypothesis that ash clogs pores to the point that infiltration rates are sufficiently reduced to generate surface runoff. In laboratory experiments, we assessed the rapidly acting factors underlying pore clogging, namely physical and chemical processes. Our first objective was to elucidate how accumulation of ash in porous media is affected by sand texture and ash thickness (Objective 1). Additional factors evaluated were rainfall rate, initial moisture content and raindrop impact. We also determined the likelihood of chemical pore clogging (Objective 2), and the saturated hydraulic conductivity for pure, mixed and layered sand–ash systems (Objective 3). Because the ash literature uses the term 'pore clogging' in the context of reduced infiltration and increased surface runoff, we define this term here as the blocking of pores such that infiltration is hampered and ponding or runoff occurs. We thereby make a clear distinction with ash washing into pores, here defined as the movement of ash into porous media regardless of any potential clogging and thus ponding effects.

Material and methods

Experimental design

Objective 1 was assessed with two sets of infiltration experiments visualised with a bright-field microscope (Fig. 1). The first set (experiment A) was performed using ash collected from a Douglas-fir (*Pseudotsuga menziesii*) stand burned in the 2010 Fourmile Canyon wildfire (Colorado, USA) where Ebel (2012) and Ebel *et al.* (2012) studied post-wildfire hydrologic and erosional responses. Using a factorial design, we tested effects of ash thickness and sand texture on ash transport (Fig. 1) near saturation. The second set of infiltration experiments (B, C and D) assessed potential pore clogging in additional scenarios (Fig. 1). Because ash transport in experiment A was limited, we tested the effect of tripling the rainfall rate (experiment B), expecting increased ash transport to increase pore-clogging potential. As post-fire rain events typically occur when soils are dry, we also performed the experiments using dry sand (experiment C). And because raindrop impact may considerably promote ash transport into soils, we additionally took raindrop impact into account (experiment D). Three replicates were done for each treatment.

Douglas-fir is a common tree species throughout western North America (Steinberg 2002), and its dense growth and moderate surface fuel loading promote high-severity fires, making hillslopes prone to post-fire runoff and erosion (Moody and Martin 2001). To place the Douglas-fir ash in a broader perspective, we analysed an additional eight wildland fire ashes that varied in physical and chemical characteristics (Table 1, Tables S1–2 in the Supplementary material (available online only), Fig. S1; see Text S1 for methods). In Objective 2, we calculated DLVO interaction energies from ζ-potentials measured for these ashes and for the sand used in Objective 1 (Fig. 1). In Objective 3, the same materials and a fine sand were analysed for saturated hydraulic conductivity. We also tested whether ash fully incorporated into the sand would reduce the hydraulic conductivity any differently from an ash layer on top of the sand (Fig. 1).

Experimental setup

Ash thickness vs sand texture infiltration experiment (A)

Three ash thicknesses and sand textures were evaluated: 0.5-, 1.0- and 2.0-cm thick ash – broadly representative of post-fire field conditions (Cerdà and Doerr 2008; Woods and Balfour 2008; Stoof *et al.* 2010), and medium sand (0.53 mm mean

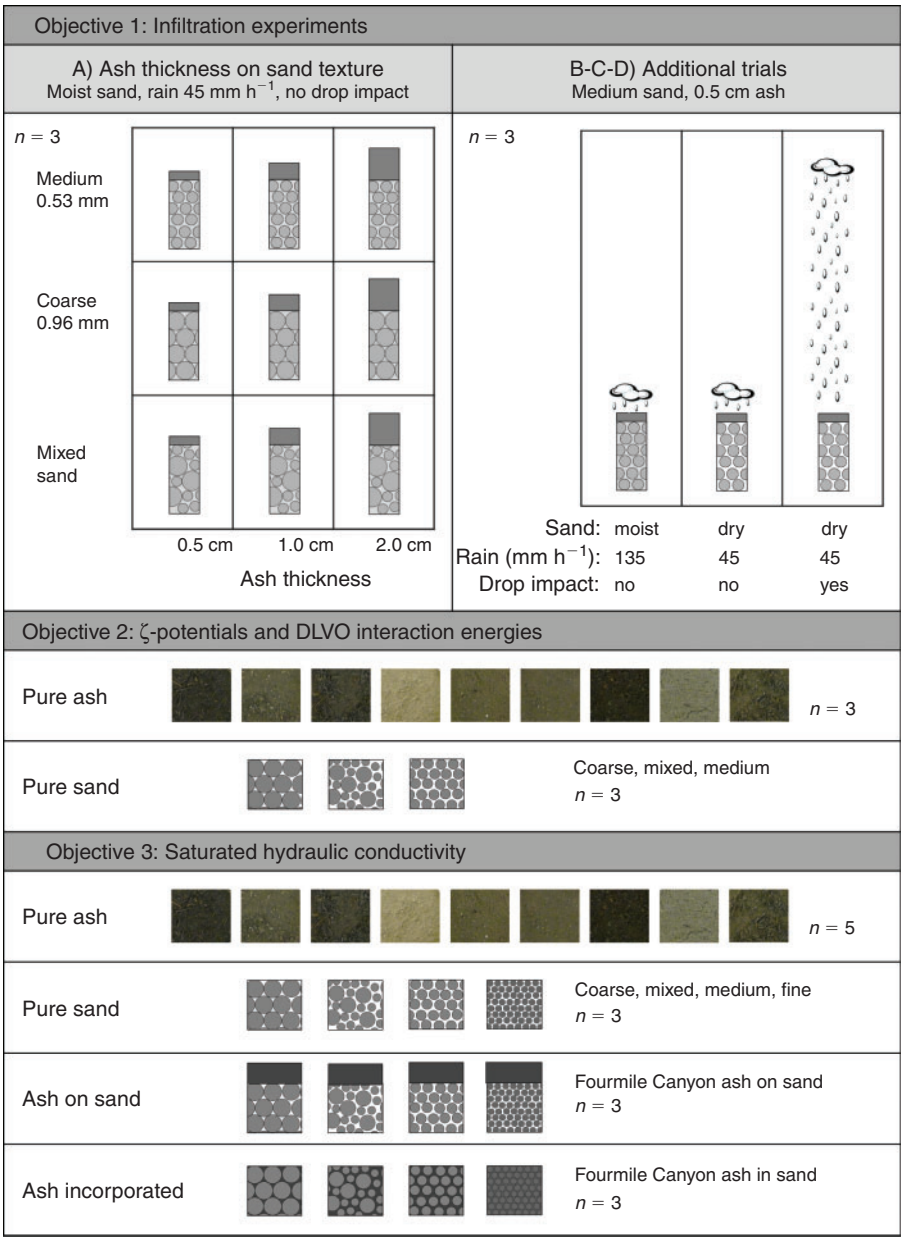

Fig. 1. Experimental design of Objectives 1, 2 and 3. DLVO, Derjaguin–Landau–Verweij–Overbeek theory.

diameter, 0.45–0.60 mm range), coarse sand (0.96 mm mean diameter, 0.85–1.15 mm range), and a 1 : 1 mixture of the two. As real soils have poor visualisation characteristics (it is hard to distinguish ash from soil), we used industrial hydrophilic quartz sand (hereafter referred to as pure sand) for its good light transmission and simple analysis of leachate. The mean pore size, determined following Arya *et al.* (1999; see also Text S1), was 0.34 mm for medium sand and 0.62 mm for coarse sand.

Infiltration experiments were performed using a transparent $2 \times 2 \times 10$-cm vertical flow cell that allowed simultaneous microscopic visualisation, broadly following Morales *et al.* (2009) and Sang *et al.* (2014). Setup details are given in Fig. S2 and Text S1. In short, the column was lined with wire mesh, wet-packed with pure sand and ash was added on top. A polyester filter was used to ensure homogeneous distribution of simulated rainfall, applied using a peristaltic pump at 45 mm h^{-1}, a rate on the high end of rainfall intensities in the Colorado Rocky Mountains (Moody and Martin 2001). Each experiment lasted 2 h, such that the entire pore volume was flushed four times under a small (3-cm) suction. Pore-scale ash transport and attachment processes were visualised *in situ* using a digital bright-field microscope (KH-7700, Hirox-USA, River Edge, NJ). Column outflow was collected at 3-min intervals and analysed for ash concentration at 590 nm using a spectrophotometer. Although some components of ash are water-soluble (Pereira *et al.* 2011), spectrophotometer analysis

Table 1. Wildland fire ashes and their origin

Ash	Species	Origin	Fire date	Comments	Munsell colour[4]	Organic matter (%)[5]	WDPT[6]	Ash texture equivalent[7]
A	Juniper (*Juniperus* spp.)	Fourmile Canyon Fire, Colorado, USA	10 Sept 2010		10YR 3/1	7.7	<5 s	'Loamy sand'
B	Douglas-fir (*Pseudotsuga menziesii*)	Fourmile Canyon Fire, Colorado, USA	10 Sept 2010	Ash from N-facing slope	10YR 3/1	5.7	<5 s	'Loamy sand'
C	Currant (*Ribes* spp.)	Fourmile Canyon Fire, Colorado, USA	10 Sept 2010	Ash from S-facing slope	10YR 2/2	13.7	<5 s	'Loamy sand'
D	Ponderosa pine (*Pinus ponderosa*) and possibly other species	Overland Fire, Colorado, USA	29 Oct 2003	Composite of wind-blown white ash and underlying black ash	10YR 3/1	4.4	<5 s	'Fine sandy loam'
E	Ponderosa pine (*Pinus ponderosa*)	Overland Fire, Colorado, USA	29 Oct 2003	Recognisable charred organic matter	10YR 2/1	20.8	>1 min	'Loamy sand'
F[1]	Aleppo pine (*Pinus halepensis*)	Prescribed fire near Reus, Spain	21 May 2004	Black ash	10YR 2/1	37.0	30 s	'Loamy sand'
G[1]	Aleppo pine (*Pinus halepensis*)	Prescribed fire near Reus, Spain	21 May 2004	White ash	10YR 5/1	12.9	12 s	'Fine sandy loam'
H[2]	Maritime pine (*Pinus pinaster*) and shrub understorey (incl. *Erica scoparia*, *Pterospartum tridentatum*, *Cytisus striatus*)	Marão River watershed, near Vila Real, Portugal	Jun 2006		10YR 3/1	41.7	<5 s	'Loamy coarse sand'
J[3]	Spruce (*Picea* spp.) and fir (*Abies* spp.)	Jocko Lakes Fire near Seeley Lake, Montana	17 Sep 2007	Very fibrous ash with filaments	10YR 6/1	9.3	<5 s	'Fine sandy loam'

[1]Ash collected by Xavi Úbeda.
[2]Ash collected by Maria Rosário Costa (Costa *et al.* 2014).
[3]Ash collected by Stefan Doerr.
[4]Classified using Munsell Color (1975).
[5]Determined by loss on ignition.
[6]Water drop penetration time.
[7]Ash texture equivalent determined in suspension following Miller and Schaetzl (2012) and USDA soil texture classification (Soil Survey Division Staff 1993).

accounts primarily for the visible particles, the absorbance of soluble ions or organics being minimal at this wavelength. The amount of ash remaining on top was calculated as the difference between the amount of ash in the initial ash layer and the amounts of ash transported into the sand and leached through the column.

After each experiment, sand was removed from the column and sectioned into 10 depth increments (Text S1) to determine ash distribution with depth. Transported ash amounts were quantified from ash concentration after adding 20 mL deionised water and quickly measuring the light absorption of its supernatant.

Second set of infiltration experiments (B, C, D)

Experiments B, C, D (Fig. 1) were performed using the same general procedure as described above, using the ash thickness and pure sand texture that showed greatest ash retention in experiment A: 0.5-cm ash and medium sand. For the high rainfall rate experiment (B), an extreme rate (Dunkerley 2008) of 135 mm h^{-1} was used. To keep the number of pore volumes flushed during a run constant, runtime was reduced to 40 min. For the dry soil experiment (C), columns were dry-packed and a rainfall rate of 45 mm h^{-1} was used. Finally, for the raindrop impact experiments (D), columns were dry-packed, the polyester filter covering the ash was omitted and 45 mm h^{-1} rainfall was applied ~0.7 m above the ash while the outlet of the hose supplying the simulated raindrops was manually shifted to create some scatter in the location of the drops. Splashing of ash was not observed.

ζ-potential and DLVO

To assess the potential for chemical clogging, we determined the likelihood of ash particles attaching to sand surfaces, which depends greatly on the surface charge of both materials. In short, we generated suspensions of ash and sand colloids (Johnson 1999; Zhang *et al.* 2010*b*) to determine their electrophoretic mobility and ζ-potentials. Then, total DLVO interaction energy was calculated as the sum of Lifshitz–van der Waals and electrical double-layer interactions. This was done for ash particles of 1 and 10 μm interacting with pure sand in water of 1 or 10 mM ionic strength. Then, theoretical attachment efficiency was calculated to quantify the tendency of ash to attach to sand (Text S1).

Effect of ash layer or incorporation on hydraulic conductivity

Saturated hydraulic conductivity was determined using the constant head method (Stolte 1997) for all nine ashes, the abovementioned medium, coarse and mixed sand, and a fine

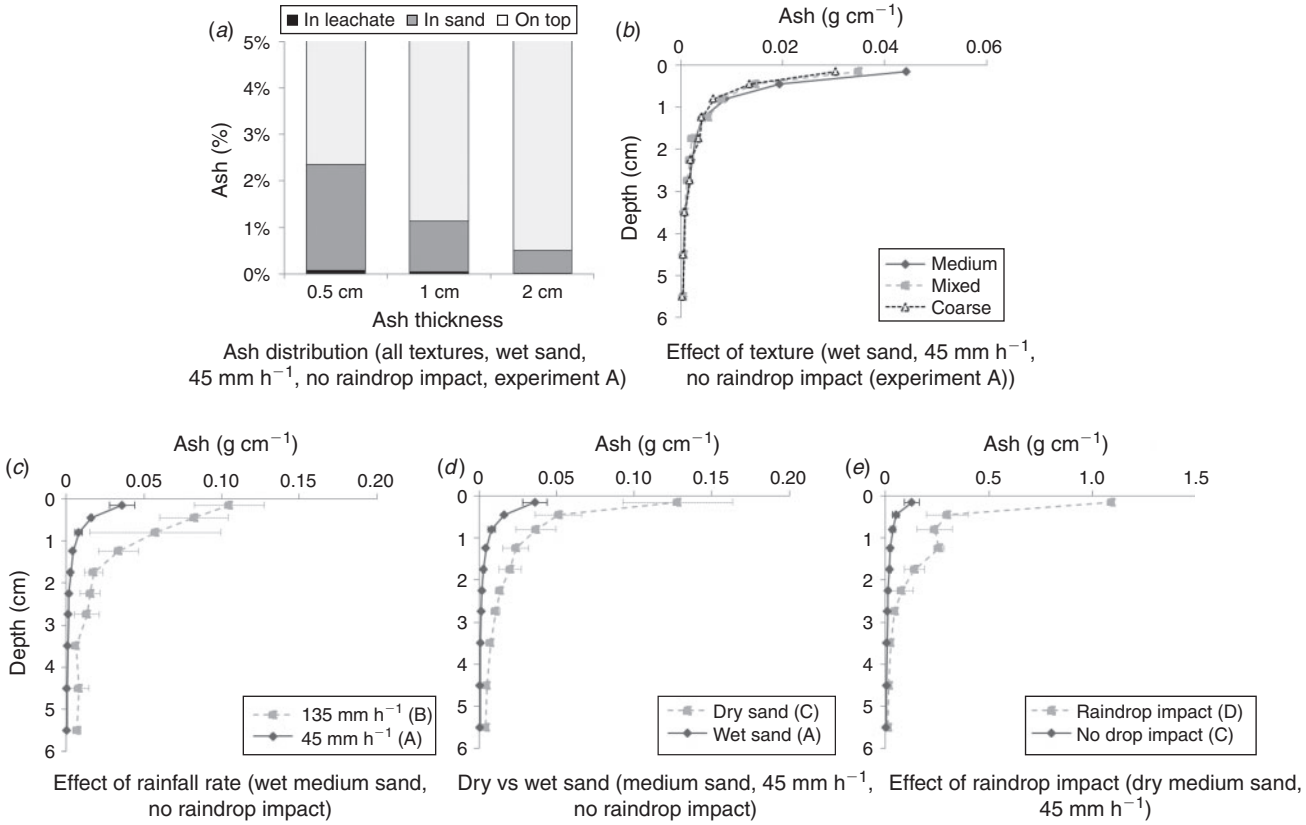

Fig. 2. Effect of ash thickness (*a*); sand texture (*b*); rainfall rate (*c*); initial sand wetness (*d*); and raindrop impact (*e*) on ash distribution. Note that the *y* axis in (*a*) is truncated, and that the scale of the *x* axes in (*b–e*) varies. Texture effects in (*b*) are only significant at 0–0.3-cm depth (significantly more ash in medium sand than in the other two textures); in (*c–e*), effects are significant for all depths.

sand (0.20 mm mean diameter, 0.08–0.30 mm range), which were analysed following Text S1. Effects of a 0.5-cm ash layer and incorporation of the same amount of ash (Table S3) were tested using Douglas-fir ash and all four sand textures. In all cases, five replicates were performed per treatment, except for Ash F and H ($n = 3$) for which little material was available.

Statistical analysis

The amount of ash in leachate, sand and on top of the sand after experiment A was analysed using two-way ANOVAs to assess significant effects of sand texture and ash thickness, for each compartment separately. One-way ANOVAs were used to assess effects of high rainfall (B), zero initial moisture (C) and raindrop impact (D). Effects on ash distribution with depth were analysed with factorial models fitted using residual maximum likelihood (Text S1). One-way ANOVAs were used for ash and sand separately to identify significant differences in saturated conductivity, organic matter, porosity, bulk density, pH, electrophoretic mobility and ζ-potential. Effects of an ash layer and ash incorporation on saturated conductivity as a function of pure sand texture were assessed with two-way ANOVA. In all cases, significant differences between treatments ($P < 0.05$) were determined using least square difference (LSD) tests, and analyses were performed in *R* (R Development Core Team 2010).

Results

Infiltration experiment A: ash thickness and sand texture

The majority of ash remained on the sand surface during the 2-h infiltration experiments, with only a small fraction of ash washing into the pure sand (0.5–2.3% of the original ash layer) and leaching out of the column (0.2–0.8%). Although the amount of ash transported into the pure sand was slightly greater for medium sand (Fig. S3) and for the 0.5-cm ash layer (Fig. 2*a*), these effects were not significant: the total amount of ash in sand after the 2-h infiltration experiments was neither affected by ash thickness ($P = 0.632$), nor by sand texture ($P = 0.356$). The percentage of ash washed into the pure sand was therefore greatest for the thinnest ash layer (Fig. 2*a*). A significant two-way interaction ($P < 0.001$) indicated that the effect of ash thickness and sand texture on ash in the column leachate was not as straightforward.

Dissection of the sand column after the experiment showed that most of the ash was located in the top 1.5 cm (Fig. 2*b*). A significant two-way interaction (sand texture × depth, $P = 0.002$) indicated that the amount of ash that was washed in sharply decreased with depth (Fig. 2*b*) and was affected by sand texture. Effects of texture were, however, only significant for the 0–0.3-cm depth, for which medium sand contained significantly more ash than coarse sand. There were also

significant two-way interactions between ash thickness and sand depth ($P = 0.036$) and ash thickness and sand texture ($P = 0.014$), but LSD analysis revealed no significant effects of ash thickness for any depth or texture combination.

Contrary to expectations, ponding of water on top of the ash did not occur during any of the experimental runs. This was despite the 45-mm h^{-1} rainfall rate applied being higher than typical rainfall intensities. Microscope images taken at and just below the ash–sand interface show that ash accumulation gradually increased during the 2-h experiments, and that most of the particles were smaller than ~0.05 mm (Fig. S4, Video S1). Although the ash particles were distributed throughout the sand matrix (i.e. not in bands; Bond 1986), their distribution was very sparse.

Infiltration experiments B, C, D

The second set of infiltration experiments evaluated the effects of increased rainfall intensity (experiment B; Video S2), zero initial sand moisture (experiment C; Video S3) and raindrop impact (experiment D, Video S4), all significantly altering the mass of ash transported into the pure sand ($P < 0.0001$), leached out of the column ($P = 0.0016$) and left on top of the pure sand ($P < 0.0001$). The 3-fold increase of rainfall intensity from experiment A to B significantly increased ash transport (Video S1), resulting in a 5.4-fold increase in the amount of ash washed into the pure sand: from 2 to 11% of the initial ash layer (Fig. 3*a*, *b*). This increase was significant for all depths but most notable in the top 1.5 cm (rainfall rate × depth interaction $P = 0.014$; Fig. 2*c*). The amount of ash in leachate also significantly increased from 0.06 to 0.20% of the initial ash layer (a 3.6-fold increase), though remaining very small at 0.025 g.

Interestingly, experiment C (zero initial moisture) resulted in equivalent ash transport to experiment B (rainfall intensity): the drop in initial sand moisture content significantly increased the amount of ash transported into the pure sand by 4.8-fold, from 2 to 10% of the initial ash layer (Fig. 3*a–c*). This increase was significant for all depths but most evident from the ash–sand interface to 1.5–2 cm deep – the zone where the majority of ash accumulated (initial moisture × depth interaction $P = 0.011$; Fig. 2*d*). Despite this increase in ash transported into the pure sand, the amount of ash in leachate did not significantly change. This may be caused by the fact that the volume leached during the dry-sand run ('C', Fig. 3) was 33% lower than during the wet-sand run ('A', Fig. 3) as it took much longer for the wetting front to reach the bottom of the column and the outflow to start (average of 42 min instead of 3 min).

Raindrop impact (experiment D) had by far the greatest effects on ash movement, compared with the other treatments. It caused a significant 6.7-fold increase in the amount of ash transported into the pure sand (from 10 to 66% of the initial ash layer). Raindrop impact also significantly increased the ash content of sand throughout the column, though most evidently down to a depth of 2–2.5 cm (raindrop impact × depth interaction $P = 0.019$; Fig. 2*e*). The amount of ash in leachate significantly increased by a factor 3.2, from 0.09 to 0.30% of the initial ash layer.

Despite the considerable increase in the amount of ash washed in for this second set of experiments (B, C, D), ponding was again not observed during any of the runs (not even for the extremely high rainfall intensity of 135 mm h^{-1}). Yet, although all water readily infiltrated into the ash, there was a delay in water being released from the ash into the underlying pure sand (Video S5). In the dry-sand experiment (C), this delay lasted ~1 min, after which the water was released into the sand for the remainder of the experiment.

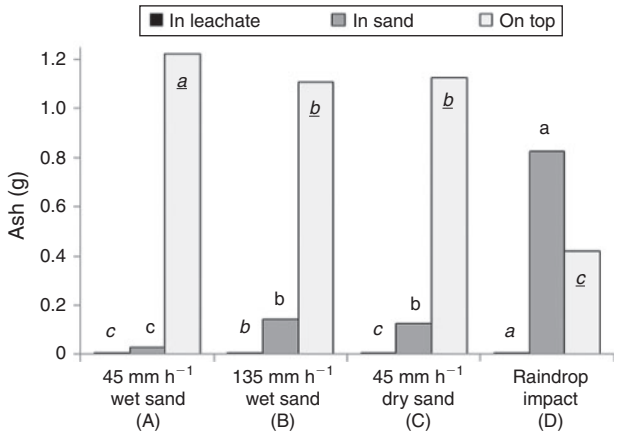

Fig. 3. Ash transport in infiltration experiments B, C, D that test the effect of rainfall rate (treatments A–B), initial sand wetness (A–C) and raindrop impact (C–D, which both have 45 mm h^{-1} rainfall rate on dry sand). All runs were done with medium sand, and treatments A through C were done without raindrop impact. Different lowercase letters in the same font (italic, regular or underlined) indicate significant differences between treatments at $P < 0.05$.

Similarly to experiment A, we did not observe any signs of pore clogging in the microscope visualisations of experiments B, C, D. Ash was again distributed throughout the sand matrix, showing both individual particles and loose clumps of particles or 'flocs'. Both the small (~0.02 mm) and larger particles or flocs (0.05–0.1 mm; Fig. 4) were very mobile. Real-time observation of flow processes furthermore showed that even when ash particles or loose flocs appeared to be fixed in a pore, they regularly disaggregated and moved position. This is illustrated in Fig. 4 and Videos S3–4. Interestingly, very small particles were even observed to pass particles or flocs that appeared to 'block' pores (Video S2), indicating that even when ash may be temporarily positioned in pores, these pores are essentially not blocked at all and water may still move through.

ζ-potential values and DLVO interaction energies

The electrophoretic mobility and ζ-potential data show that all sands and ash types evaluated had broadly similar negative surface charge (Table S4). As indicated by DLVO interaction energy profiles (Fig. S5), there was an overall unfavourable interaction between the colloidal ash particles (<10 μm, 5% of all ash) and pure sand surfaces. Despite these overall unfavourable conditions for attachment in so-called primary minima, these very small ash particles may be loosely retained in secondary minima. The latter attachment increases with particle size and ionic strength of the pore water (Text S1).

Hydraulic conductivity

Saturated conductivity of the pure wildland fire ashes (K_{ash}) ranged between 31 and 147 mm h^{-1}, approximately an order of

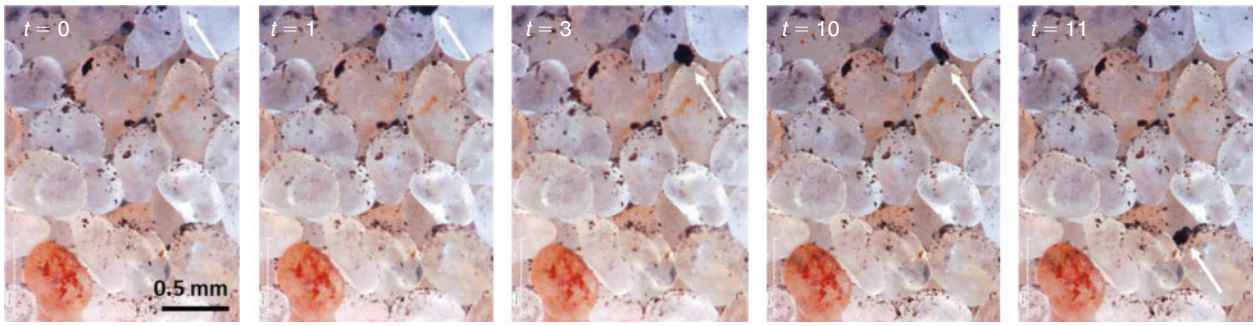

Fig. 4. Example of movement of a large ash particle from the high-rainfall-rate experiment B (wet sand, medium texture with 0.5-cm ash layer, 135-mm h^{-1} rainfall rate), with t indicating the time from the start of this sequence of images. At $t = 0$ min (left panel), the pore in the upper right corner is empty; after 1 min, the ash particle has appeared that after 3 min is located in the pore underneath. For 6 min, the particle seems rather stuck in this pore, but it then moves ($t = 10$ min) and quickly washes down to a pore 1 mm deeper ($t = 11$ min).

Table 2. Saturated hydraulic conductivity (K_{sat}) of the pure wildland fire ashes and pure sands

Values not sharing the same letter (lowercase for ash, uppercase for sand) for a given material (ash or sand) are significantly different at $P < 0.05$

Ash or sand	K_{sat} (mm h^{-1})	
Ash A	92 ± 16	ab
Ash B	147 ± 50	a
Ash C	116 ± 62	ab
Ash D	31 ± 7	b
Ash E	140 ± 36	a
Ash F	42 ± 16	ab
Ash G	103 ± 11	ab
Ash H	58 ± 11	ab
Ash J	93 ± 20	ab
Coarse sand	1615 ± 99	A
Mixed sand[1]	1360 ± 194	B
Medium sand	1250 ± 121	B
Fine sand	691 ± 104	C

[1]Mixed sand here is a 1 : 1 mix of coarse and medium sand.

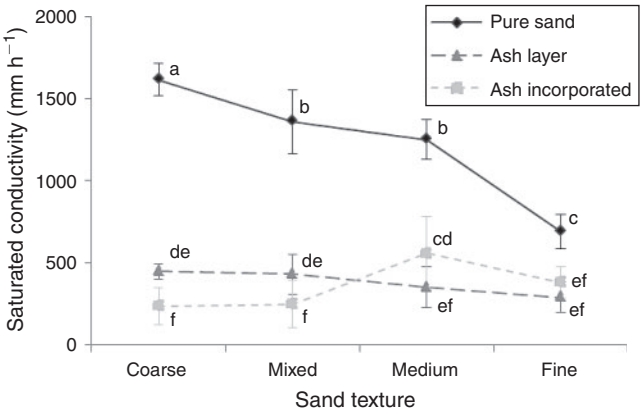

Fig. 5. Effect of a 0.5-cm-thick layer of Douglas-fir ash and incorporation of the same amount of ash on the saturated hydraulic conductivity of four sand textures, with error bars indicating ±1 s.d. Values not sharing the same lowercase letter are significantly different at $P < 0.05$.

magnitude lower than the very high conductivity of the pure sands evaluated ($K_{porous\ media}$, 691–1615 mm h^{-1}, Table 2). As indicated by the significant interaction ($P < 0.0001$) between sand texture and ash arrangement and illustrated in Fig. 5, effects of ash layer and incorporation were strongest for the coarser textures. Interestingly, a layer of ash had broadly similar effects to incorporation of the same amount of ash (Fig. 5). Incorporation of 0.5 cm ash into 3 cm sand significantly reduced the K_{sat} of the material by a factor 2 to 7 (depending on the texture of the pure sand) from ~690–1600 to 240–560 mm h^{-1}. Addition of the same amount of ash as a layer on top of the pure sand significantly reduced the saturated conductivity of the system 2 to 4-fold from ~690–1600 to 290–450 mm h^{-1}.

Discussion

Ash transport

In line with previous experiments (Stoof *et al.* 2010), a considerable fraction to almost the majority of the ash remained on the surface during the infiltration experiments (Fig. 3). We found no significant effect of sand texture on total ash transport in experiment A (Fig. 2*b*, S3). This contrasts with the findings of Woods and Balfour (2010) from thin sections taken after rainfall experiments in the field, which showed more ash particles in coarse than in fine-textured soil. The lack of texture effects in our experiments may be explained by the relation between the particle size distribution of the ash and the pore size of our pure sands, which suggests that washing in of ash was not very restricted: 72% of ash was smaller than the mean pore diameter of the medium sand, and 89% of ash was smaller than the mean pore diameter of the coarse sand (Fig. S1). The sandy loam and loamy sand studied by Woods and Balfour (2010) were much finer than our pure sands, suggesting that a pore size threshold may exist (between sandy loam and loamy sand) controlling whether ash particles can wash into soils. As transport of fine particles into coarser material is a function of the particle size ratio of both materials (Wu and Huang 2000; Tan *et al.* 2003), this pore size threshold for downward ash transport likely varies with ash particle size. A major difference between the present study and Woods and Balfour (2010) is also that the latter study was done in the field, where poorer textural sorting (B. Ebel, pers. comm.) and soil organic matter may have facilitated straining of ash particles. Raindrop impact, which significantly

increases ash transport (Figs 2–3), is another explanation, and may accentuate soil texture effects.

Of all the factors considered (ash thickness, sand texture, rainfall rate, initial moisture and raindrop impact), raindrop impact had by far the greatest effect on ash movement. This strong effect of raindrop impact may not only be ascribed to raindrops more easily entraining ash particles than gently infiltrating water, but also to increased force pushing ash particles into the pure sand. In the video observations (Supplemental material), this raindrop impact shows in pulses of markedly increased ash transport (Video S4). Surprisingly, the decrease of initial sand moisture content from near-saturation to zero also had significant effects (Figs 2–3). This may be because ash transport was not only enhanced by fluctuations in water flow in saturated pores (Video S1–2), but because ash was also temporarily immobilised along the edges of air bubbles (Video S3), ash transport was additionally facilitated by the movement of air–water interfaces (see also Saiers *et al.* 2003; Zhuang *et al.* 2010). Although the bulk of the Douglas-fir ash is hydrophilic (Table 1), these particles were probably hydrophobic (e.g. Bodí *et al.* 2011), as they preferred the air–water interface. When the air bubbles burst, the attached particles were released back into the pore water (Video S3), markedly enhancing ash transport. Even though raindrop impact can also generate air bubbles and thereby cause similar effects, this was not observed.

Mobility of ash is also very sensitive to transient water fluxes such as the raindrop impact-related steady intermittent movement of pore water at ~10-s intervals (Video S4), and to a lesser degree the fluxes caused by the more infrequent swapping of the cuvette collecting the leachate. The latter experimental setup effects are often ignored in explaining colloid retention but are common (Zevi *et al.* 2006; Dathe *et al.* 2014) and therefore should be investigated more. Interestingly, the regular pulsing caused by raindrops was also seen in dry sand without raindrop impact (Video S3), suggesting that even gentle application of water drops on ash slightly increases flow rates and facilitates ash transport.

Physical and chemical pore clogging

Microscope observations of real-time infiltration (Fig. 4, S4, Videos S1–S5) supported quantitative evidence (Figs 2, 3, S3) that ash was transported into the pure sands. Despite frequent assumptions in field experiments (Etiégni and Campbell 1991; Nyman *et al.* 2010; Woods and Balfour 2010; Bodí *et al.* 2012; Bodí *et al.* 2014), widespread pore clogging was not observed and ponding did not occur during any of our laboratory experiments. We observed an interesting balance between the washing in of ash and its mobilisation with rainfall rate. With increased infiltration or rainfall rate, not only the total ash transport (Figs 2–3) but also the pore-scale water flow rate increased. Although having more ash would suggest a higher pore-clogging potential, the increased flow in pores essentially reduces the likelihood of clogging because of increased particle mobility (Bradford and Torkzaban 2008). In general, very little ash washed into the pure sand, and ash particles or flocs were often located in pore necks (at the grain–grain contact, Fig. 4) and at the air–water interface (Video S3). These loosely attached ash particles and flocs were rather mobile (Fig. 4, Videos S3–4) with small particles even being able to pass pores in which ash flocs were (temporarily) located (Video S2). Any ash located in pore necks therefore seems temporary, and not completely blocking water flow. This indicates that even if individual pores are actually blocked, significant overall permeability changes are unlikely owing to (1) the small fraction of pores affected by the low amount of ash transported into the sand; (2) water flow pathways in porous media not being straight but inherently tortuous (Vervoort and Cattle 2003; Cai and Yu 2011; Video S2) such that even when one pore is blocked the water can go somewhere else; and (3) the quite high saturated conductivity of pure ash and ash–sand mixtures (Table 2; Bodí *et al.* 2014), indicating that even 'blocked' pores may be rather water permeable.

The unlikeliness of pore clogging by ash is supported by the fact that pronounced electrostatic attraction of ash to sand is improbable, as both materials have an overall negative surface charge (Table S4). For colloidal ash (<10 μm), generally unfavourable deposition onto the pure sand surface is expected based on DLVO theory (Fig. S5). Although this applies to our smallest 5% of particles only, based on video observations (Supplemental material), it is not expected that the larger particles attach either. Despite these overall unfavourable conditions for attachment in primary minima, weak attachment is expected at secondary minima that becomes increasingly strong with ash particle size or pore-water ionic strength. Nevertheless, even weak attachment of ash does not appear to block water flow, as can be seen in Video S2 and in other studies (Zhang *et al.* 2010*a*; Sang *et al.* 2013).

As field soils and organic matter are also negatively charged above pH ~3 (Kretzschmar and Sticher 1997; Fernández Marcos *et al.* 1998; Taubaso *et al.* 2004), electrostatic repulsion of ash is likely also the case in most field situations. A limited degree of electrostatic attraction may however occur for soil particles coated with metal oxides that are positively charged (Fernández Marcos *et al.* 1998; Wang *et al.* 2013). Such positively charged patches may serve as favourable retention microsites for negatively charged ash, facilitating potential attachment of ash in pores.

Hydrologic implications

The observation that much ash does not wash into sand or soil (Figs 2, 3; Stoof *et al.* 2010), indicates its susceptibility to aboveground relocation by water and wind, and the vulnerability of surface waters to ash contamination. The ash that does wash in is distributed in a steep gradient with depth (Fig. 2), suggesting that soil hydraulic changes due to ash such as increased water retention (Stoof *et al.* 2010; Ebel 2012) are limited to the upper few centimetres. The exact depth will likely depend on ash, soil and rainfall characteristics, and initial soil moisture content at the time of the rain event.

It is important to note that the laboratory experiments discussed here all evaluated the effects of a first and single rainfall event. Although potential pore clogging by ash has been used to explain surface runoff after the first post-fire rains (e.g. Woods and Balfour 2010), clogging of porous media typically takes several weeks to months of infiltration to become fully effective and cause ponding (Blazejewski and Murat-Blazejewska 1997; Platzer and Mauch 1997; Baveye *et al.* 1998; Wu and Huang 2000), depending among other things on

the characteristics of the porous medium and the overlying fine material (e.g. particle size distribution, porosity), the flow rate through the porous medium, and the availability of the fine material. In the case of ash, both ash characteristics and immobilisation can be considerably affected by drying and wetting cycles occurring between rain events. Wetting and subsequent drying of ash can for instance markedly change its mineralogical composition (Bodí *et al.* 2012), which may cause severe crust formation (Balfour *et al.* 2014). Like raindrop impact (Video S4), intermittent drying and wetting can increase ash transport during the wetting phase, as ash may irreversibly attach to the sand during the drying phase like colloids do, when the meniscus dries out. Potential effects of multiple wetting and drying effects therefore remain to be investigated, for different types of ash.

Alternative hydrologic effects of ash

The experiments described here evaluated whether pore clogging by ash can explain post-fire runoff. Yet, as recognised by others (e.g. Meixner and Wohlgemuth 2003; Larsen *et al.* 2009; Moody and Ebel 2012; Stoof *et al.* 2012), increased post-fire runoff and erosion are not caused by one single factor, but rather the interaction of several factors. Post-fire infiltration may be reduced by surface sealing but also by fire-induced changes in soil texture and aggregate stability, or by increased soil water repellency (Martin and Moody 2001; Larsen *et al.* 2009; Mataix-Solera *et al.* 2011; Stoof *et al.* 2011). Although our findings demonstrate that pore clogging of ash in pure sand is unlikely responsible for surface runoff, our data offer three alternative mechanisms by which ash affects post-fire hydrology, all related to fine-on-coarse systems: (1) saturated conductivity differences; (2) delay of water release from ash; and (3) ash overlying water-repellent soil.

Considering saturated conductivity, simply having a layer of ash can considerably reduce permeability of fine to coarse sands (Fig. 5). This reduction is in line with very basic theories for water flow (Fetter 2000), and is similar to the effects of soil water repellency on infiltration (e.g. Fox *et al.* 2007; Nyman *et al.* 2010). The impact of this ash layer is a function of the permeability of both ash and the underlying porous medium (pure sand in the present study, soil in field situations). For two-layer systems where $K_{ash} < K_{porous\ medium}$, K_{ash} will reduce overall permeability such that $K_{total} < K_{porous\ medium}$. This is, for example, the case for our highly permeable pure sands (Fig. 5) and when our ashes overlie sandy soils (210 mm h^{-1}; Rawls *et al.* 1982). In the field, the exact reduction will be determined by a range of factors, including the amount of ash present, its permeability, the permeability of the underlying soil, the degree to which ash has washed into the soil, and the hydrophobicity of the ash. In the case of our Douglas-fir ash overlying Rawls *et al.*'s (1982) 210-mm h^{-1} sandy soil, the reduction is probably smaller than the 2 to 7-fold reductions observed for the more permeable pure sands in Fig. 5. For two-layer systems where $K_{ash} > K_{porous\ medium}$, overall permeability will not be limited by ash, such that $K_{total} \approx K_{porous\ medium}$. This is the case for extremely permeable ash (720 or 3600 mm h^{-1}; Bodí *et al.* 2014) and for low-permeability soils such as loams and clays (13.2 and 0.6 mm h^{-1} respectively; Rawls *et al.* 1982). As the saturated conductivity of ash is typically not that extreme, but rather 56–165 mm h^{-1} (Bodí *et al.* 2014), $K_{ash} > K_{porous\ medium}$ situations caused by extremely permeable ash are likely rare and will probably mostly occur because of low soil permeability. The high K_{ash} values also indicate that infiltration excess runoff from ash will generally occur during rain events of extreme intensity; yet, as reported by Ebel *et al.* (2012), it can still occur when ash permeability is very low (8.6 mm h^{-1}).

The delay of water release from the ash into the underlying sand (Video S5) is typical for fine-on-coarse layered systems, and is caused by the difference in pore sizes of both layers. Such textural interfaces can form capillary barriers (Smesrud and Selker 2001; Kinner and Moody 2010) that hold percolating water in the fine-grained layer by capillary forces (Steenhuis *et al.* 1991; Schroth *et al.* 1998). Water in unsaturated porous media does not flow through the largest pores but rather through the smallest pores possible, owing to the fact that a lower pressure is required for water to flow into a small pore than a large pore. As capillary forces hold water in the fine top layer in fine-on-coarse systems, water pressure builds up until it exceeds the air entry value required to flow into the larger pores in the layer underneath (Baker and Hillel 1990; Steenhuis *et al.* 1991). Flow below capillary barriers can be highly unstable, typically inducing preferential finger flow even in fully homogeneously textured and structured media (Baker and Hillel 1990; Steenhuis *et al.* 1991). This ash-induced preferential flow can explain the irregular soil-wetting patterns found by Bodí *et al.* (2012) under ash layers, and cause preferential leaching of infiltrated water to deeper layers (Ritsema and Dekker 1995), increasing base flow. By inducing preferential flow due to these capillary barrier effects, ash layers may contribute to the increase in streamflow volumes (Stoof *et al.* 2014) that are commonly observed post-fire (Scott 1997; Stoof *et al.* 2012).

More relevant to surface runoff, capillary barriers can also cause lateral flow through the fine top layer (Ross 1990; Steenhuis *et al.* 1991), as previously observed in ash layers (Kinner and Moody 2010; Bodí *et al.* 2012) and soils (Ross 1990; Schroth *et al.* 1998) and utilised in hydraulic isolation of waste (Smesrud and Selker 2001). The spatial extent of this lateral flow is in the order of metres (Ross 1990), with flow occurring in the unsaturated ash until the combined effect of rainfall and lateral flow cause the suction in the ash layer to exceed the air entry value of the coarser soil. Although capillary barrier effects thereby may explain the occurrence of *unsaturated* flow in ash-on-coarse soil systems, they cannot explain *saturated* flow through such ash layers without taking soil water repellency into account. Infiltration into wettable soils, which have negative air entry pressures (Baker and Hillel 1990), will already occur when ash is unsaturated. This is in contrast to water-repellent soils, which have positive air entry pressures (Wang *et al.* 2000) and therefore require ponding (and thus saturation) to allow water infiltration. Capillary barrier effects caused by a layer of fine ash over coarse soil may therefore only cause saturation excess runoff when the underlying soil is water repellent.

Conclusions

In infiltration and visualisation experiments using ash overlying sand, only small quantities of ash were transported into the pure sand or leached out, with the majority remaining on the surface.

Transport of ash into the pure sand was most increased by raindrop impact, and similarly increased for completely dry sand. Although these experiments confirm field and laboratory observation of ash presence in pores, physical clogging of pores to the point that water infiltration is blocked and ponding occurs was not observed. Chemical clogging by attachment to pure sand particles is also unlikely, given the negative charge of ash and sand. And finally, because of high saturated conductivity, ash will generally be able to absorb also the highest rainfall intensities, even when mixed with or transported into porous media. This suggests that pore clogging is an unlikely cause of surface runoff from sands. Although these small-scale laboratory experiments using pure sand do not account for the full complexity of processes occurring in field soils (e.g. the presence of organic matter, water repellency, surface charge heterogeneity), the fundamental mechanisms described here regarding physical and chemical clogging processes are instrumental in understanding the fate of ash in more complex systems. This study is therefore a first step towards analysing ash transport and attachment processes in field soils. Additional research into how interactions between ash, soil and rainfall characteristics affect soil hydrology can further elucidate the drivers and impacts of ash transport in the field. This is not only relevant from a hydrological perspective, but also to understand potential effects of ash on soils (Badía *et al.* 2014; Rubio 2014), carbon sequestration and water quality in burned areas.

Acknowledgements

We thank Douglas Caveney for constructing the flow chambers, Elliot Friedman for providing the wire mesh, and Xavi Úbeda, Maria do Rosário Melo da Costa and Stefan Doerr for supplying some of the wildland fire ashes, Peter J. Vermeulen and Brian Ebel for discussion, Christian Munoz for assistance with the HIROX microscope, Keith J. Lucey for proofreading, and Randall Schaetzl for determining particle size distribution of the ash. We also thank the participants of the AGU Chapman conference 'Synthesizing empirical results to improve predictions of post-wildfire runoff and erosion responses' for scenarios to test to get ash to clog pores, such as by using dry sand and raindrop impact. This work was partially supported by an International Association of Wildland Fire Scholarship (C.R.S.) and an Agriculture and Food Research Initiative Competitive grant no. 2013–67019–21377 from the USDA National Institute of Food and Agriculture. Any use of trade, firm, or product names is for descriptive purposes only and does not imply endorsement by the US Government.

References

Arya LM, Leij FJ, van Genuchten MT, Shouse PJ (1999) Scaling parameter to predict the soil water characteristic from particle-size distribution data. *Soil Science Society of America Journal* **63**, 510–519. doi:10.2136/SSSAJ1999.03615995006300030013X

Audry S, Akerman A, Riotte J, Oliva P, Marechal J-C, Fraysse F, Pokrovsky OS, Braun J-J (2014) Contribution of forest fire ash and plant litter decay on stream dissolved composition in a sub-humid tropical watershed (Mule Hole, southern India). *Chemical Geology* **372**, 144–161. doi:10.1016/J.CHEMGEO.2014.02.016

Badía D, Martí C, Aguirre AJ, Aznar JM, González-Pérez JA, De la Rosa JM, León J, Ibarra P, Echeverría T (2014) Wildfire effects on nutrients and organic carbon of a Rendzic Phaeozem in NE Spain: changes at cm-scale topsoil. *Catena* **113**, 267–275. doi:10.1016/J.CATENA.2013.08.002

Baker RS, Hillel D (1990) Laboratory tests of a theory of fingering during infiltration into layered soils. *Soil Science Society of America Journal* **54**, 20–30. doi:10.2136/SSSAJ1990.03615995005400010004X

Balfour VN, Woods SW (2013) The hydrological properties and the effects of hydration on vegetative ash from the Northern Rockies, USA. *Catena* **111**, 9–24. doi:10.1016/J.CATENA.2013.06.014

Balfour VN, Doerr SH, Robichaud PR (2014) The temporal evolution of wildfire ash and implications for post-fire infiltration. *International Journal of Wildland Fire* **23**, 733–745. doi:10.1071/WF13159

Baveye P, Vandevivere P, Hoyle BL, DeLeo PC, de Lozada DS (1998) Environmental impact and mechanisms of the biological clogging of saturated soils and aquifer materials. *Critical Reviews in Environmental Science and Technology* **28**, 123–191. doi:10.1080/10643389891254197

Blazejewski R, Murat-Blazejewska S (1997) Soil clogging phenomena in constructed wetlands with subsurface flow. *Water Science and Technology* **35**, 183–188. doi:10.1016/S0273-1223(97)00067-X

Bodí MB, Mataix-Solera J, Doerr SH, Cerdà A (2011) The wettability of ash from burned vegetation and its relationship to Mediterranean plant species type, burn severity and total organic carbon content. *Geoderma* **160**, 599–607. doi:10.1016/J.GEODERMA.2010.11.009

Bodí MB, Doerr SH, Cerdà A, Mataix-Solera J (2012) Hydrological effects of a layer of vegetation ash on underlying wettable and water-repellent soil. *Geoderma* **191**, 14–23. doi:10.1016/J.GEODERMA.2012.01.006

Bodí MB, Martin DA, Balfour VN, Santín C, Doerr SH, Pereira P, Cerdà A, Mataix-Solera J (2014) Wildland fire ash: production, composition and ecohydrogeomorphic effects. *Earth-Science Reviews* **130**, 103–127. doi:10.1016/J.EARSCIREV.2013.12.007

Bond WJ (1986) Illuvial band formation in a laboratory column of sand. *Soil Science Society of America Journal* **50**, 265–267. doi:10.2136/SSSAJ1986.03615995005000010054X

Bradford SA, Torkzaban S (2008) Colloid transport and retention in unsaturated porous media: a review of interface-, collector-, and pore-scale processes and models. *Vadose Zone Journal* **7**, 667–681. doi:10.2136/VZJ2007.0092

Bradford SA, Morales VL, Zhang W, Harvey RW, Packman AI, Mohanram A, Welty C (2013) Transport and fate of microbial pathogens in agricultural settings. *Critical Reviews in Environmental Science and Technology* **43**, 775–893. doi:10.1080/10643389.2012.710449

Cai J, Yu B (2011) A discussion of the effect of tortuosity on the capillary imbibition in porous media. *Transport in Porous Media* **89**, 251–263. doi:10.1007/S11242-011-9767-0

Cerdà A, Doerr SH (2008) The effect of ash and needle cover on surface runoff and erosion in the immediate post-fire period. *Catena* **74**, 256–263. doi:10.1016/J.CATENA.2008.03.010

Cerdà A, Robichaud P (Eds) (2009) Fire effects on soils and restoration strategies. In 'Land reconstruction and management series, Vol. 5'. (Science Publishers: Enfield, NH). doi:10.1201/9781439843338-F

Costa MR, Calvão AR, Aranha J (2014) Linking wildfire effects on soil and water chemistry of the Marão River watershed, Portugal, and biomass changes detected from Landsat imagery. *Applied Geochemistry* **44**, 93–102. doi:10.1016/J.APGEOCHEM.2013.09.009

Dathe A, Zevi Y, Richards BK, Gao B, Parlange J-Y, Steenhuis TS (2014) Functional models for colloid retention in porous media at the triple line. *Environmental Science and Pollution Research International* **21**, 9067–9080. doi:10.1007/S11356-013-2120-0

De Vries J (1972) Soil filtration of wastewater effluent and the mechanism of pore clogging. *Journal – Water Pollution Control Federation* **44**, 565–573.

Dlapa P, Bodí MB, Mataix-Solera J, Cerdà A, Doerr SH (2013) FT-IR spectroscopy reveals that ash water repellency is highly dependent on ash chemical composition. *Catena* **108**, 35–43. doi:10.1016/J.CATENA.2012.02.011

Dunkerley D (2008) Rain event properties in nature and in rainfall simulation experiments: a comparative review with recommendations for increasingly systematic study and reporting. *Hydrological Processes* **22**, 4415–4435. doi:10.1002/HYP.7045

Ebel BA (2012) Wildfire impacts on soil-water retention in the Colorado Front Range, United States. *Water Resources Research* **48**, W12515. doi:10.1029/2012WR012362

Ebel BA, Moody JA, Martin DA (2012) Hydrologic conditions controlling runoff generation immediately after wildfire. *Water Resources Research* **48**, WR011470. doi:10.1029/2011WR011470

Etiégni L, Campbell AG (1991) Physical and chemical characteristics of wood ash. *Bioresource Technology* **37**, 173–178. doi:10.1016/0960-8524(91)90207-Z

Fernández Marcos ML, Buurman P, Meijer EL (1998) Role of organic matter and sesquioxides on variable charge of three soils from Galicia, Spain. *Communications in Soil Science and Plant Analysis* **29**, 2441–2457. doi:10.1080/00103629809370123

Fetter CW (2000) 'Applied hydrogeology.' (Prentice Hall: Upper Saddle River, NJ)

Fox DM, Darboux F, Carrega P (2007) Effects of fire-induced water repellency on soil aggregate stability, splash erosion, and saturated hydraulic conductivity for different size fractions. *Hydrological Processes* **21**, 2377–2384.

Gabet EJ, Sternberg P (2008) The effects of vegetative ash on infiltration capacity, sediment transport, and the generation of progressively bulked debris flows. *Geomorphology* **101**, 666–673. doi:10.1016/J.GEOMORPH.2008.03.005

Giglio L, Randerson JT, van der Werf GR, Kasibhatla PS, Collatz GJ, Morton DC, DeFries RS (2010) Assessing variability and long-term trends in burned area by merging multiple satellite fire products. *Biogeosciences* **7**, 1171–1186. doi:10.5194/BG-7-1171-2010

Goforth BR, Graham RC, Hubbert KR, Zanner CW, Minnich RA (2005) Spatial distribution and properties of ash and thermally altered soils after high-severity forest fire, southern California. *International Journal of Wildland Fire* **14**, 343–354. doi:10.1071/WF05038

Hubbert KR, Preisler HK, Wohlgemuth PM, Graham RC, Narog MG (2006) Prescribed burning effects on soil physical properties and soil water repellency in a steep chaparral watershed, southern California, USA. *Geoderma* **130**, 284–298. doi:10.1016/J.GEODERMA.2005.02.001

Johnson PR (1999) A comparison of streaming and microelectrophoresis methods for obtaining the ζ potential of granular porous media surfaces. *Journal of Colloid and Interface Science* **209**, 264–267. doi:10.1006/JCIS.1998.5908

Kinner DA, Moody JA (2010) Spatial variability of steady-state infiltration into a two-layer soil system on burned hillslopes. *Journal of Hydrology* **381**, 322–332. doi:10.1016/J.JHYDROL.2009.12.004

Kretzschmar R, Sticher H (1997) Transport of humic-coated iron oxide colloids in a sandy soil: influence of Ca^{2+} and trace metals. *Environmental Science & Technology* **31**, 3497–3504. doi:10.1021/ES970244S

Kutiel P, Lavee H, Segev M, Benyamini Y (1995) The effect of fire-induced surface heterogeneity on rainfall–runoff–erosion relationships in an eastern Mediterranean ecosystem, Israel. *Catena* **25**, 77–87. doi:10.1016/0341-8162(94)00043-E

Larsen IJ, MacDonald LH, Brown E, Rough D, Welsh MJ, Pietraszek JH, Libohova Z, de Dios Benavides-Solorio J, Schaffrath K (2009) Causes of post-fire runoff and erosion: water repellency, cover, or soil sealing? *Soil Science Society of America Journal* **73**, 1393–1407. doi:10.2136/SSSAJ2007.0432

León J, Bodí MB, Cerdà A, Badía D (2013) The contrasted response of ash to wetting: the effects of ash type, thickness and rainfall events. *Geoderma* **209–210**, 143–152. doi:10.1016/J.GEODERMA.2013.06.018

Mallik AU, Gimingham CH, Rahman AA (1984) Ecological effects of heather burning. I. Water infiltration, moisture retention and porosity of the surface soil. *Journal of Ecology* **72**, 767–776. doi:10.2307/2259530

Martin DA, Moody JA (2001) Comparison of soil infiltration rates in burned and unburned mountainous watersheds. *Hydrological Processes* **15**, 2893–2903. doi:10.1002/HYP.380

Mataix-Solera J, Cerdà A, Arcenegui V, Jordán A, Zavala LM (2011) Fire effects on soil aggregation: a review. *Earth-Science Reviews* **109**, 44–60. doi:10.1016/J.EARSCIREV.2011.08.002

McDowell-Boyer LM, Hunt JR, Sitar N (1986) Particle transport through porous media. *Water Resources Research* **22**, 1901–1921. doi:10.1029/WR022I013P01901

Meixner T, Wohlgemuth PM (2003) Climate variability, fire, vegetation recovery, and watershed hydrology. In 'First interagency conference on research in the watersheds', 27–30 October 2003, Benson, AZ. (Eds KG Renard, SA McElroy, WJ Gburek, EH Canfield, RL Scott) (USDA Agricultural Research Service: Benson, AZ)

Miller BA, Schaetzl RJ (2012) Precision of soil particle size analysis using laser diffractometry. *Soil Science Society of America Journal* **76**, 1719–1727. doi:10.2136/SSSAJ2011.0303

Moody JA, Ebel BA (2012) Hyper-dry conditions provide new insights into the cause of extreme floods after wildfire. *Catena* **93**, 58–63. doi:10.1016/J.CATENA.2012.01.006

Moody JA, Martin DA (2001) Initial hydrologic and geomorphic response following a wildfire in the Colorado Front Range. *Earth Surface Processes and Landforms* **26**, 1049–1070. doi:10.1002/ESP.253

Moody JA, Shakesby RA, Robichaud PR, Cannon SH, Martin DA (2013) Current research issues related to post-wildfire runoff and erosion processes. *Earth-Science Reviews* **122**, 10–37. doi:10.1016/J.EARSCIREV.2013.03.004

Morales VL, Gao B, Steenhuis TS (2009) Grain surface-roughness effects on colloidal retention in the vadose zone. *Vadose Zone Journal* **8**, 11–20. doi:10.2136/VZJ2007.0171

Munsell Color (1975) 'Munsell soil color charts.' (Macbeth, a division of Kollmorgen Corporation: Baltimore, MD)

Nyman P, Sheridan G, Lane PNJ (2010) Synergistic effects of water repellency and macropore flow on the hydraulic conductivity of a burned forest soil, south-east Australia. *Hydrological Processes* **24**, 2871–2887. doi:10.1002/HYP.7701

Nyman P, Sheridan GJ, Smith HG, Lane PNJ (2014) Modeling the effects of surface storage, macropore flow and water repellency on infiltration after wildfire. *Journal of Hydrology* **513**, 301–313. doi:10.1016/J.JHYDROL.2014.02.044

Onda Y, Dietrich WE, Booker F (2008) Evolution of overland flow after a severe forest fire, Point Reyes, California. *Catena* **72**, 13–20. doi:10.1016/J.CATENA.2007.02.003

Pereira P, Úbeda X, Martin D, Mataix-Solera J, Guerrero C (2011) Effects of a low-severity prescribed fire on water-soluble elements in ash from a cork oak (*Quercus suber*) forest located in the north-east of the Iberian Peninsula. *Environmental Research* **111**, 237–247. doi:10.1016/J.ENVRES.2010.09.002

Pereira P, Úbeda X, Martin DA (2012) Fire severity effects on ash chemical composition and water-extractable elements. *Geoderma* **191**, 105–114. doi:10.1016/J.GEODERMA.2012.02.005

Pereira P, Cerdà A, Úbeda X, Mataix-Solera J, Arcenegui V, Zavala LM (2015) Modelling the impacts of wildfire on ash thickness in a short-term period. *Land Degradation and Development* **26**, 180–192. doi:10.1002/LDR.2195

Pereira P, Cerdà A, Úbeda X, Mataix-Solera J, Martin D, Jordán A, Burguet M (2013*b*) Spatial models for monitoring the spatiotemporal evolution of ashes after fire – a case study of a burnt grassland in Lithuania. *Solid Earth* **4**, 153–165. doi:10.5194/SE-4-153-2013

Platzer C, Mauch K (1997) Soil clogging in vertical flow reed beds – mechanisms, parameters, consequences and... solutions? *Water Science and Technology* **35**, 175–181. doi:10.1016/S0273-1223(97)00066-8

R Development Core Team (2010) *R*: A language and environment for statistical computing. (R Foundation for Statistical Computing: Vienna, Austria) Available at www.R-project.org [Verified 3 November 2015]

Rawls WJ, Brakensiek DL, Saxtonn KE (1982) Estimation of soil water properties. *Transactions of the ASAE* **25**, 1316–1320. doi:10.13031/2013.33720

Ritsema CJ, Dekker LW (1995) Distribution flow: a general process in the top layer of water-repellent soils. *Water Resources Research* **31**, 1187–1200. doi:10.1029/94WR02979

Ross B (1990) The diversion capacity of capillary barriers. *Water Resources Research* **26**, 2625–2629. doi:10.1029/WR026I010P02625

Rubio CM (2014) Short-term change in the thermal conductivity of a loam soil after forest fire. *European Journal of Environmental and Safety Sciences* **2**, 28–36. Available at http://www.sci-institute.com/2014_volume_2_issue_2/rubio.pdf [Verified 27 October 2015]

Saiers JE, Hornberger GM, Gower DB, Herman JS (2003) The role of moving air–water interfaces in colloid mobilization within the vadose zone. *Geophysical Research Letters* **30**, 2083. doi:10.1029/2003GL018418

Sang W, Morales VL, Zhang W, Stoof CR, Gao B, Schatz AL, Zhang Y, Steenhuis TS (2013) Quantification of colloid retention and release by straining and energy minima in variably saturated porous media. *Environmental Science & Technology* **47**, 8256–8264.

Sang W, Stoof CR, Zhang W, Morales VL, Gao B, Kay RW, Liu L, Zhang Y, Steenhuis TS (2014) Effect of hydrofracking fluid on colloid transport in the unsaturated zone. *Environmental Science & Technology* **48**, 8266–8274. doi:10.1021/ES501441E

Santín C, Doerr SH, Shakesby RA, Bryant R, Sheridan GJ, Lane PN, Smith HG, Bell TL (2012) Carbon loads, forms and sequestration potential within ash deposits produced by wildfire: new insights from the 2009 'Black Saturday' fires, Australia. *European Journal of Forest Research* **131**, 1245–1253. doi:10.1007/S10342-012-0595-8

Schroth MH, Istok JD, Selker JS (1998) Three-phase immiscible fluid movement in the vicinity of textural interfaces. *Journal of Contaminant Hydrology* **32**, 1–23. doi:10.1016/S0169-7722(97)00069-7

Scott DF (1997) The contrasting effects of wildfire and clearfelling on the hydrology of a small catchment. *Hydrological Processes* **11**, 543–555. doi:10.1002/(SICI)1099-1085(199705)11:6<543::AID-HYP474>3.0.CO;2-J

Shakesby RA, Doerr SH (2006) Wildfire as a hydrological and geomorphological agent. *Earth-Science Reviews* **74**, 269–307. doi:10.1016/J.EARSCIREV.2005.10.006

Smesrud JK, Selker JS (2001) Effect of soil-particle size contrast on capillary barrier performance. *Journal of Geotechnical and Geoenvironmental Engineering* **127**, 885–888. doi:10.1061/(ASCE)1090-0241(2001)127:10(885)

Smith HG, Sheridan GJ, Lane PNJ, Nyman P, Haydon S (2011) Wildfire effects on water quality in forest catchments: a review with implications for water supply. *Journal of Hydrology* **396**, 170–192. doi:10.1016/J.JHYDROL.2010.10.043

Soil Survey Division Staff (1993) 'Soil survey manual', Handbook 18. (United States Department of Agriculture: Washington, DC) Available at http://www.nrcs.usda.gov/wps/portal/nrcs/detail/soils/ref/?cid=nrcs142p2_054262 [Verified 17 November 2015]

Steenhuis TS, Parlange JY, Kung KJS (1991) Comment on 'The diversion capacity of capillary barriers' by Benjamin Ross. *Water Resources Research* **27**, 2155–2156. doi:10.1029/91WR01366

Steinberg PD (2002) *Pseudotsuga menziesii* var. *glauca*. In 'Fire Effects Information System' [online database]. USDA Forest Service, Rocky Mountain Research Station, Fire Sciences Laboratory. Available at http://feis-crs.org/beta/ [Verified 3 November 2015]

Stolte J (1997) Determination of the saturated hydraulic conductivity using the constant head method. In 'Manual for soil physical measurements, version 3, Technical Document 37'. (Ed. J Stolte) pp. 27–32. (DLO – Staring Centre: Wageningen, The Netherlands)

Stoof CR, Wesseling JG, Ritsema CJ (2010) Effects of fire and ash on soil water retention. *Geoderma* **159**, 276–285. doi:10.1016/J.GEODERMA.2010.08.002

Stoof CR, Moore D, Ritsema CJ, Dekker LW (2011) Natural and fire-induced soil water repellency in a Portuguese shrubland. *Soil Science Society of America Journal* **75**, 2283–2295. doi:10.2136/SSSAJ2011.0046

Stoof CR, Vervoort RW, Iwema J, van den Elsen E, Ferreira AJD, Ritsema CJ (2012) Hydrological response of a small catchment burned by experimental fire. *Hydrology and Earth System Sciences* **16**, 267–285. doi:10.5194/HESS-16-267-2012

Stoof CR, Slingerland EC, Mol W, van den Berg J, Vermeulen PJ, Ferreira AJD, Ritsema CJ, Parlange JY, Steenhuis TS (2014) Preferential flow as a potential mechanism for fire-induced increase in streamflow. *Water Resources Research* **50**, 1840–1845. doi:10.1002/2013WR014397

Tan S-A, Fwa T-F, Han C-T (2003) Clogging evaluation of permeable bases. *Journal of Transportation Engineering* **129**, 309–315. doi:10.1061/(ASCE)0733-947X(2003)129:3(309)

Taubaso C, Dos Santos Afonso M, Torres Sánchez RM (2004) Modelling soil surface charge density using mineral composition. *Geoderma* **121**, 123–133. doi:10.1016/J.GEODERMA.2003.11.005

Vervoort R, Cattle S (2003) Linking hydraulic conductivity and tortuosity parameters to pore space geometry and pore-size distribution. *Journal of Hydrology* **272**, 36–49. doi:10.1016/S0022-1694(02)00253-6

Wang D, Zhang W, Zhou D (2013) Antagonistic effects of humic acid and iron oxyhydroxide grain-coating on biochar nanoparticle transport in saturated sand. *Environmental Science & Technology* **47**, 5154–5161. doi:10.1021/ES305337R

Wang Z, Wu L, Wu Q (2000) Water-entry value as an alternative indicator of soil water-repellency and wettability. *Journal of Hydrology* **231–232**, 76–83. doi:10.1016/S0022-1694(00)00185-2

Woods SW, Balfour VN (2008) The effect of ash on runoff and erosion after a severe forest wildfire, Montana, USA. *International Journal of Wildland Fire* **17**, 535–548. doi:10.1071/WF07040

Woods SW, Balfour VN (2010) The effects of soil texture and ash thickness on the post-fire hydrological response from ash-covered soils. *Journal of Hydrology* **393**, 274–286. doi:10.1016/J.JHYDROL.2010.08.025

Wu F-C, Huang H-T (2000) Hydraulic resistance induced by deposition of sediment in porous medium. *Journal of Hydraulic Engineering* **126**, 547–551. doi:10.1061/(ASCE)0733-9429(2000)126:7(547)

Zevi Y, Dathe A, Gao B, Richards BK, Steenhuis TS (2006) Quantifying colloid retention in partially saturated porous media. *Water Resources Research* **42**, W12S03. doi:10.1029/2006WR004929

Zhang W, Morales VL, Cakmak ME, Salvucci AE, Geohring LD, Hay AG, Parlange J-Y, Steenhuis TS (2010*a*) Colloid transport and retention in unsaturated porous media: effect of colloid input concentration. *Environmental Science & Technology* **44**, 4965–4972. doi:10.1021/ES100272F

Zhang W, Niu J, Morales VL, Chen X, Hay AG, Lehmann J, Steenhuis TS (2010*b*) Transport and retention of biochar particles in porous media: effect of pH, ionic strength, and particle size. *Ecohydrology* **3**, 497–508. doi:10.1002/ECO.160

Zhuang J, Goeppert N, Tu C, McCarthy J, Perfect E, McKay L (2010) Colloid transport with wetting fronts: interactive effects of solution surface tension and ionic strength. *Water Research* **44**, 1270–1278. doi:10.1016/J.WATRES.2009.12.012